



Flow-measurements of the viscosity coefficients of two nematic liquid crystalline azoxybenzenes

W.W. Beens, W.H. de Jeu

► To cite this version:

W.W. Beens, W.H. de Jeu. Flow-measurements of the viscosity coefficients of two nematic liquid crystalline azoxybenzenes. Journal de Physique, 1983, 44 (2), pp.129-136. 10.1051/jphys:01983004402012900 . jpa-00209578

HAL Id: jpa-00209578

<https://hal.science/jpa-00209578>

Submitted on 4 Feb 2008

HAL is a multi-disciplinary open access archive for the deposit and dissemination of scientific research documents, whether they are published or not. The documents may come from teaching and research institutions in France or abroad, or from public or private research centers.

L'archive ouverte pluridisciplinaire **HAL**, est destinée au dépôt et à la diffusion de documents scientifiques de niveau recherche, publiés ou non, émanant des établissements d'enseignement et de recherche français ou étrangers, des laboratoires publics ou privés.

LE JOURNAL DE PHYSIQUE

J. Physique **44** (1983) 129-136

FÉVRIER 1983, PAGE 129

Classification
Physics Abstracts
47.15 — 47.62

Flow-measurements of the viscosity coefficients of two nematic liquid crystalline azoxybenzenes

W. W. Beens and W. H. de Jeu

Solid State Physics Laboratory, University of Groningen, Melkweg 1, 9718 EP Groningen, The Netherlands

(Reçu le 2 août 1982, accepté le 14 octobre 1982)

Résumé. — On a construit un appareil pour mesurer les viscosités de cisaillement η_1 , η_2 , η_3 et η_{12} de Miesowicz. Celles-ci sont déterminées lors de l'écoulement d'un liquide nématique dans un capillaire rectangulaire qui fait partie d'un appareil thermostatisé. L'ensemble est situé entre les pôles d'un électro-aimant pour contrôler le directeur \mathbf{n} . De plus, on a déterminé l'angle d'alignement par écoulement en mesurant la variation de la biréfringence dans l'échantillon entre la situation où \mathbf{n} est fixé parallèle à l'écoulement et celle où il est aligné par l'écoulement. On donne des résultats pour des ensembles complets de coefficients de viscosité de p-méthoxy-p'-butylazoxybenzène et de p, p'-dibutylazoxybenzène. Les résultats sont bien en accord avec des rapports visco-élastiques obtenus par des techniques de diffusion de la lumière. La relation d'Onsager-Parodi est bien vérifiée compte tenu de la précision expérimentale.

Abstract. — To determine the Miesowicz viscosity coefficients a shear-flow set-up has been built, which allows the measurement of η_1 , η_2 , η_3 and η_{12} . These coefficients are determined by pressing the liquid crystal through a rectangular capillary which forms part of a thermostated set-up placed between the poles of a magnet in order to control the director \mathbf{n} . In addition, the flow-alignment angle θ_0 is determined from the change in optical path difference between the ordinary and extraordinary components of polarized light, comparing the situation with \mathbf{n} aligned along the flow-direction and with flow-alignment, respectively. Results are given for the complete set of viscosity coefficients of p-methoxy-p'-butylazoxybenzene and p, p'-dibutylazoxybenzene. The results show good agreement with visco-elastic ratios found with light-scattering techniques. Within the experimental accuracy the Onsager-Parodi relation is well fulfilled.

1. Introduction. — Though a nematic liquid crystal flows as easily as a conventional organic liquid consisting of similar molecules, an analysis of the viscosities turns out to be rather complicated when the state of alignment (given by the director \mathbf{n}) is considered. In the first place, the flow depends on the angles between \mathbf{n} and the flow direction and the velocity gradient. Secondly, translational motions couple to inner orientational motions, and the flow will cause the director to rotate. This behaviour can be described by the hydrodynamic theory of Ericksen and Leslie [1], which involves six viscosity coefficients, of which five are independent [2].

Experimentally the direction of \mathbf{n} must be controlled

and/or measured, and conventional viscometric equipment is of little use. This is probably the cause that in spite of the importance of the viscosities for the dynamics of many physical effects (including the switching times of display devices) experiments that can be quantitatively interpreted are relatively scarce. Only recently some authors [3, 4, 6] have started systematic measurements again. Nevertheless, to obtain for a given compound a complete set of coefficients (if possible at all) one has to rely on data from various sources which often do not seem to be compatible [5]. The only exceptions are recent results by Knepe *et al.* [6-8].

In this paper we describe in some detail the viscous

behaviour of two nematic liquid crystals : p-methoxy-p'-butylazoxybenzene (N4) and p,p'-dibutylazoxybenzene (DIBAB). Four coefficients (η_1 , η_2 , η_3 and η_{12} , to be defined below) are obtained from shear-flow experiments in a magnetic field. In addition the flow-alignment angle θ_0 is determined in a separate experiment, while moreover the rotational viscosity γ_1 is obtained from the dynamics of the Frederiks' transition for twist. This latter type of measurement will be described in detail elsewhere [9]. The two compounds are chosen such that a comparison can be made with results for visco-elastic ratios obtained by Van Eck *et al.* [10] using light-scattering techniques.

2. Theory. — **2.1 MIESOWICZ VISCOSITIES.** — We consider a simple shear-flow between two flat plates forming a rectangular capillary. Immediately three relevant geometries are evident (see Fig. 1) that give a viscosity coefficient and a sheart-torque coefficient. The latter describes the torque on the director due to the shear :

- (a) $\mathbf{n} \parallel \nabla \mathbf{v}$: viscosity η_1 , shear-torque coefficient κ_1 .
- (b) $\mathbf{n} \parallel \mathbf{v}$: viscosity η_2 , shear-torque coefficient κ_2 .
- (c) $\mathbf{n} \perp (\mathbf{v}, \nabla \mathbf{v})$: viscosity η_3 , no shear-torque coefficient.

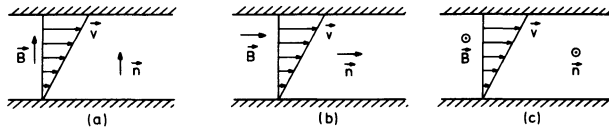


Fig. 1. — (a) Geometry for the measurement of η_1 and κ_1 ; (b) Geometry for the measurement of η_2 and κ_2 ; (c) Geometry for the measurement of η_3 .

We have followed here the notation of Helfrich [11, 12]. In the original paper by Miesowicz [13] the definitions of η_1 and η_2 are interchanged. Apart from the shears depicted in figure 1 that are anti-symmetric in x and z , also a coefficient η_{12} exists that is symmetric in these coordinates. It cannot be visualized in a pure shear, but appears in the general expression for the effective viscosity η_{eff} [2] when \mathbf{n} makes an arbitrary angle with \mathbf{v} and $\nabla \mathbf{v}$ (see Fig. 2) :

$$\eta_{\text{eff}} = (\eta_1 + \eta_{12} \cos^2 \theta) \sin^2 \theta \cos^2 \phi + \eta_2 \cos^2 \theta + \eta_3 \sin^2 \theta \sin^2 \phi. \quad (1)$$

As we see the maximum contribution of η_{12} is found if \mathbf{n} is in the shear-plane at an angle of 45° with \mathbf{v} .

The volume flow rate I for a liquid with viscosity η through a rectangular capillary with length l , thickness d and width b is [14]

$$I = \frac{bd^3}{12\eta l} \left[1 - \frac{192}{\pi^5} \frac{d}{b} \right] \Delta p = c_1 \frac{\Delta p}{\eta}, \quad (2)$$

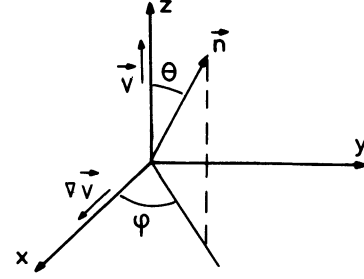


Fig. 2. — Definition of the orientation of the director with respect to the shear plane.

where c_1 is a geometrical factor and Δp is the pressure difference over the capillary. Higher order terms in d/b have been disregarded. In the experiment the liquid crystal flows through the capillary due to a pressure difference created between two gas-filled volumes on each side of the capillary, respectively. In this system the two volumes V_1 and V_2 are at pressures p_1 and p_2 , respectively. If the flow starts at $t = 0$ then the pressure difference at a time t will be

$$\Delta p(t) = p_1(t) - p_2(t), \quad (3)$$

and the volumes will be

$$V_1(t) = V_1(0) + \Delta V(t), \quad (4a)$$

$$V_2(t) = V_2(0) - \Delta V(t), \quad (4b)$$

where $\Delta V > 0$ indicates that the flow direction is from V_1 towards V_2 . Using

$$p(t) V(t) = p(0) V(0) \quad (5)$$

we can now express $\Delta p(t)$ as a function of $V_1(0)$, $V_2(0)$, $p_1(0)$, $p_2(0)$ and $\Delta V(t)$. Taking into account that $\Delta V(t) \ll V_1(0)$ and $|V_1(0) - V_2(0)| \ll V_1(0)$ we find

$$\Delta p(0) - \Delta p(t) = \{ (p_1(0) V_1(0) + p_2(0) V_2(0)) / (V_1(0) V_2(0)) \} \Delta V(t) = c_2 \Delta V(t). \quad (6)$$

The constant c_2 depends only on the initial conditions.

Knowing that $\Delta V(t) = \int_0^t I dt$, we can use relations (2)

and (6) to find

$$\Delta p(t) = \Delta p(0) \exp(-ct/\eta) \quad (7)$$

where $c = c_1 c_2$. This allows us to calculate the viscosity coefficient η from the measurement of $\Delta p(t)$.

In order to be able to interpret a specific η_{eff} , the orientation of the director must be controlled, for example by an external magnetic field. For the magnetic inductions \mathbf{B} used in practice, and for typical values of an elastic constant K and of the diamagnetic anisotropy $\Delta\chi$, the magnetic coherence length $\xi = (K\mu_0/\Delta\chi)^{1/2}/B$ is of the order of a few μm . The

misalignment due to wall effects and thus the influence of elastic torques is confined to small layers of this thickness close to the walls. They can be disregarded in comparison to the total thickness d . With the magnetic field in the shear-plane then two types of torques on the director of the flowing liquid crystal are left :

(a) The torque density N_m exerted by the magnetic induction \mathbf{B} , given by

$$N_m = \frac{1}{2} \mu_0^{-1} \Delta\chi B^2 \sin 2\psi, \quad (8)$$

where ψ is the angle between \mathbf{B} and \mathbf{n} .

(b) The torque density N_s from the shear :

$$N_s = -(\kappa_1 \sin^2 \theta + \kappa_2 \cos^2 \theta) \frac{\partial v}{\partial x}. \quad (9)$$

In equilibrium $N_m + N_s = 0$. Taking the magnetic field parallel to the x -axis (see Fig. 2), we find that for a large magnetic field θ is close to 90° and

$$\operatorname{tg} \theta = \frac{\Delta\chi B^2}{\mu_0 \kappa_1 \frac{\partial v}{\partial x}}. \quad (10)$$

In the case of a large magnetic field along the z -direction we have $\theta \approx 0$ and find similarly :

$$\operatorname{tg} \theta = \frac{-\mu_0 \kappa_2 \frac{\partial v}{\partial x}}{\Delta\chi B^2}. \quad (11)$$

The expression for the velocity gradient $\partial v / \partial x$ can be derived from

$$v(x) = v_0 \left(1 - \frac{4x^2}{d^2} \right) = \frac{\Delta p d^2}{8 l \eta_{\text{eff}}} \left(1 - \frac{x^2}{d^2} \right). \quad (12)$$

From the equations above and equation (1) one can estimate, for a certain magnetic field strength, the maximum pressure difference Δp that can be used without disturbing the uniform alignment appreciably.

2.2 FLOW-ALIGNMENT. — The total torque from the shear-flow on the director \mathbf{n} , when it is in the shear-plane, is given by equation (9). In principle this allows for an equilibrium situation at which $N_s = 0$. This occurs for the angle θ_0 , the flow-alignment angle, given by

$$\operatorname{tg}^2 \theta_0 = -\kappa_2 / \kappa_1. \quad (13)$$

Often $|\kappa_2| \ll \kappa_1$, resulting in values for θ_0 close to zero. If $\kappa_2 / \kappa_1 > 0$ no solution for θ_0 exists and the flow is not stable [3, 15, 16]. From thermodynamic considerations one finds that for rod-like molecules $\kappa_1 > 0$ [17], so that these instabilities are due to a positive sign of κ_2 .

Following Gähwiler [3] θ_0 can be determined from the change in optical path difference between the

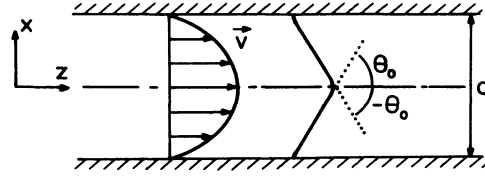


Fig. 3. — Flow-alignment in a flat capillary.

ordinary and extraordinary components of polarized light by comparing the situation with \mathbf{n} magnetically aligned along \mathbf{v} and without a magnetic field, respectively. For \mathbf{n} parallel to the z -axis (see Fig. 3), the optical path difference Γ_0 will be

$$\Gamma_0 = (n_e - n_o) d, \quad (14)$$

n_o and n_e being the ordinary and extraordinary refractive indices, respectively. When \mathbf{n} makes an angle $\theta(x)$ with the z -axis, the optical path difference Γ will be

$$\Gamma = \int_{-d/2}^{d/2} [n(\theta) - n_o] dx \quad (15)$$

with

$$\frac{1}{n^2(\theta)} = \frac{\sin^2 \theta}{n_o^2} + \frac{\cos^2 \theta}{n_e^2}. \quad (16)$$

Without a magnetic field one can have a stable situation where the total shear-torque N_s is zero. For sufficiently large shear-rates $\theta(x)$ tends to the value θ_0 , except for thin transition layers at the boundaries and in the middle. In that situation $\theta(x)$ will be given by (see Fig. 3)

$$\theta(x) = \begin{cases} \theta_0, & x > 0, \\ -\theta_0, & x < 0. \end{cases}$$

For small values of θ_0 ($\sin^2 \theta_0 \ll 1$) the change in the optical path difference is

$$\Delta\Gamma = -\frac{1}{2} n_e d \left[\left(\frac{n_e}{n_o} \right)^2 - 1 \right] \sin^2 \theta_0. \quad (17)$$

3. Experimental. — **3.1 SHEAR-FLOW.** — For the shear-flow measurement a commercially obtainable rectangular flow capillary (Hellma Küvette 136-OS) with a cross section of 0.20×9.0 mm is used. At the beginning and at the end of this type of capillary the flow direction is not parallel or orthogonal to the magnetic field (see Fig. 4). Therefore cut-outs have been made at both ends of the capillary so that these regions can be disregarded. This leaves an effective length of 27.8 mm. The two parts of the flow-cell are glued together. This causes the thickness d of the capillary to increase to a value slightly larger than the specified 0.200 ± 0.005 mm. Knowledge of the exact value of d is required, because d appears to

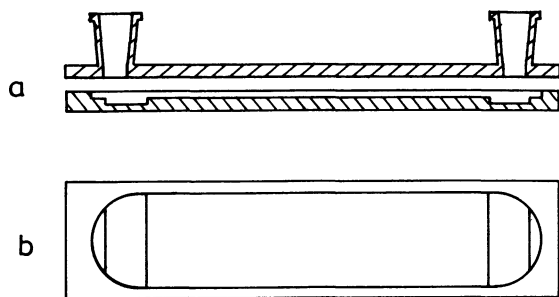


Fig. 4. — (a) Side-view of the top and of the lower part of the rectangular capillary; (b) Top-view of the lower part of the rectangular capillary.

the third power in the equations for the viscosity. Therefore d is determined by using two methods : directly by optical interference, and indirectly by measuring the viscosity of reference oils (Bendix no. 27 and no. 152). Typical results from both methods are $d = 0.204 \pm 0.002$ mm and $d = 0.205 \pm 0.002$ mm respectively, which shows that no further corrections are needed.

For each of the four viscosity coefficients (η_1 , η_2 , η_3 and η_{12}) a module has been constructed. For each module a brass holder keeps the capillary at the right position in the magnetic field (see Fig. 5). These modules fit into a heated chamber between the poles

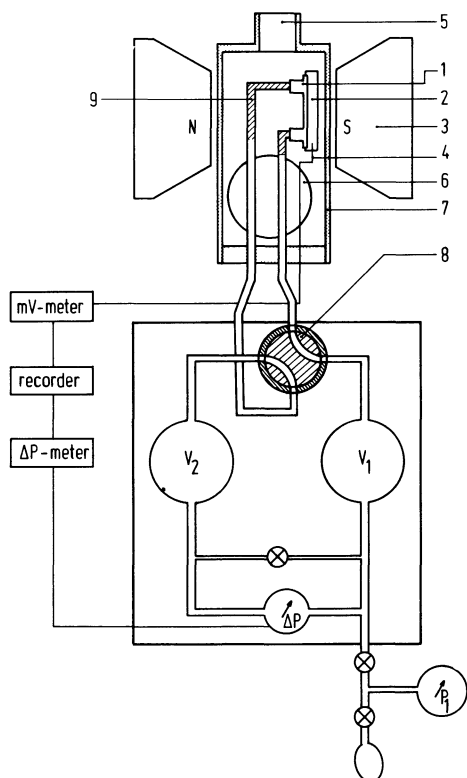


Fig. 5. — Top-view of the set-up for the shear-flow measurements; 1-capillary, 2-brass-holder, 3-magnet, 4-thermocouple, 5-hot air in, 6-hot air out, 7-heated chamber, 8-valve to change pressure direction, 9-liquid crystal.

of the magnet. The walls of this chamber are electrically heated to a temperature somewhat below the required temperature and the final temperature inside the chamber is regulated with a hot air stream. The air is circulated from the heated chamber to a heat exchanger, which is connected to a constant temperature bath. Temperatures from 15 °C up to 80 °C have been obtained with an accuracy of 0.2 °C. The temperature is measured with a thermocouple that is fixed to the brass holder of the capillary. The magnet is a Bruker BE15 with a gap of 54 mm and pole caps of 60 mm diameter, that can provide a magnetic field of 1.1 tesla.

The capillary is connected to a pressure difference system *via* two glass tubes. To avoid hydrostatic pressure differences the levels of the liquid in the glass tubes are always kept in the same horizontal plane. The pressure difference system consists of two large volumes ($V \approx 2 \times 10^{-3}$ m³), an electronic manometer, and a valve to change the direction of the pressure difference over the capillary (see Fig. 5). The electronic manometer (Datametrics, Barocel 590/1400) is used to determine the pressure difference over the capillary. It has a capacitive sensing element and can measure pressure differences from -1000 Pa to 1000 Pa. The total diaphragm displacement, with full range pressure applied, is only 0.16×10^{-6} m³. For the range used in practice (50-200 Pa) the accuracy is 0.05 %. To avoid pressure differences due to temperature differences between the volumes V_1 and V_2 , the whole set-up is placed in a box in which the temperature is kept constant. A second manometer gives the total pressure in V_1 . At the beginning of each measurement a pressure difference of about 100 Pa is created manually. The actual measurement then consist of successive readings of the pressure difference and the thermo-voltage, which are recorded on tape at fixed time intervals for automatic data-handling.

3.2 FLOW-ALIGNMENT. — The module for η_2 is designed with holes so that a laser beam can pass through the sample, which is fitted with crossed polarizers at an angle of 45° with the flow-direction. At the start of a measurement the maximum magnetic field is applied to align \mathbf{n} parallel to the flow-direction. Then the field is switched-off, the angle θ changes from zero to the flow-alignment angle θ_0 , and the related change in the intensity of the laser beam is recorded as a function of time. From the change in optical path difference, equation (17), we can calculate the flow-alignment angle. The best result is achieved with a relatively thick capillary, 500 μ m in our case.

4. Results. — When measuring the Miesowicz coefficients the director \mathbf{n} is aligned by a magnetic field. Two effects might disrupt the uniform orientation of \mathbf{n} :

(a) In the situation corresponding to η_1 or η_2 , the shear-torque tries to misalign the director.

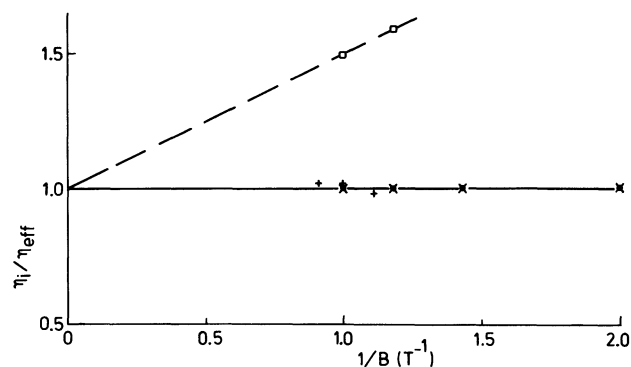


Fig. 6. — Influence of the boundary condition on the viscosities of DIBAB at 27.7 °C; (\square) η_1 without dope; (+) η_1 with dope for homeotropy (CTAB); (\bullet) η_2 ; (\times) η_3 .

(b) Due to the boundary conditions a boundary layer may exist in which the director does not have the required direction.

The first effect is determined by the values of the magnetic field and the pressure difference (Eq. (10) and (11)). The magnet has a maximum field of 1.1 T and we use a pressure difference of 100 Pa or less. With these values we calculate that in the worst case this leads to an increase of 0.5 % in the value of η_1 , and will be of no significance in the case of η_2 . The correction for η_1 given by Knepe *et al.* [6] assuming $\eta_2 = \eta_{12} = 0$ gives a similar result.

The second problem is the surface-alignment. Knepe *et al.* [6] assumed that due to boundary conditions at the surface of the capillary there is a boundary layer with viscosity η_s , while the bulk layer has the required viscosity η_i . With this division into two regions they calculated :

$$\frac{1}{\eta_i^{\text{eff}}} = \frac{1}{\eta_i} + \frac{\text{const.}}{B} \left(\frac{1}{\eta_s} - \frac{1}{\eta_i} \right), \quad i = 1, 2, 3, \quad (18)$$

with η_i^{eff} being the measured viscosity. If one plots $1/\eta_i^{\text{eff}}$ against $1/B$ one can find η_i by extrapolating to $1/B = 0$ (see Fig. 6). Another possibility to avoid

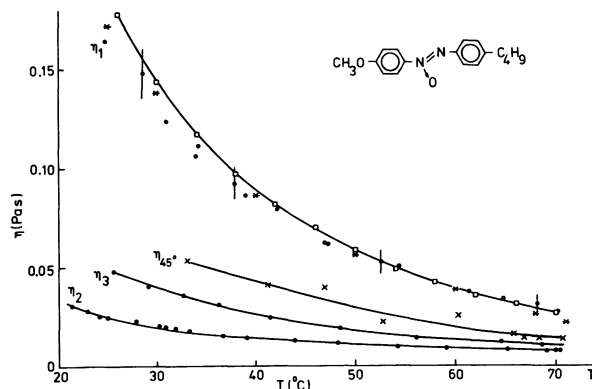


Fig. 7. — Shear-viscosities of N4; (\square) η_1 calculated via equation (21); (*) Knepe *et al.* [7].

alignment problems is to give the surface of the capillary the proper boundary conditions. For the case of η_1 a dope, 0.1 % cetyltrimethylammonium-bromide (CTAB) [ref. 2b, Ch. 2] was added to the liquid crystal to get homeotropic boundary conditions. Results for the case of DIBAB with and without this dope are shown in figure 6 together with the results for η_2 and η_3 .

The results of the measurements of the Miesowicz coefficients of N4 and DIBAB are given in figures 7 and 8. For η_2 and η_3 they can also be found in tables I

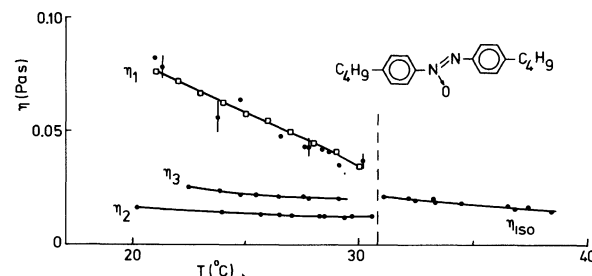


Fig. 8. — Shear-viscosities of DIBAB; (\square) η_1 calculated via equation (21).

Table I. — Results for the viscosities of N4 ($T_c = 73.8$ °C, γ_1 from [9], η_1 calculated via eq. (21)).

T (°C)	η_2 (Pa.s)	η_3 (Pa.s)	η_{45° (Pa.s)	θ_0	γ_1 (Pa.s)	η_1 (Pa.s)
26	0.024	0.047	—	4.2°	0.152	0.178
30	0.021	0.040	—	4.3°	0.122	0.144
34	0.017	0.034	0.051	4.5°	0.099	0.117
38	0.015	0.028	0.044	4.7°	0.081	0.097
42	0.013	0.025	0.039	5.1°	0.067	0.081
46	0.012	0.021	0.034	5.5°	0.056	0.069
50	0.011	0.018	0.030	6.1°	0.046	0.058
54	0.010	0.015	0.027	6.8°	0.038	0.049
58	0.009	0.013	0.023	7.7°	0.032	0.042
62	0.008	0.012	0.019	8.8°	0.026	0.035
66	0.007	0.011	0.015	10.4°	0.022	0.031
70	0.007	0.010	0.013	13.2°	0.017	0.026

Table II. — Results for the viscosities of DIBAB ($T_c = 30.8^\circ\text{C}$, γ_1 from [9], η_1 calculated via eq. (21)).

$T (^\circ\text{C})$	$\eta_2 (\text{Pa} \cdot \text{s})$	$\eta_3 (\text{Pa} \cdot \text{s})$	θ_0	$\gamma_1 (\text{Pa} \cdot \text{s})$	$\eta_1 (\text{Pa} \cdot \text{s})$
21	0.016 0	—	5.5°	0.059	0.076
22	0.015 5	—	6.0°	0.055	0.072
23	0.015 0	0.025 0	6.7°	0.051	0.067
24	0.014 5	0.023 5	7.5°	0.046	0.063
25	0.014 0	0.023 0	8.3°	0.042	0.058
26	0.014 0	0.022 0	9.5°	0.038	0.055
27	0.013 5	0.021 5	10.5°	0.034	0.050
28	0.013	0.021 0	12.0°	0.029	0.045
29	0.013	0.020 5	13.6°	0.024	0.041
30	0.013	0.020 0	16.0°	0.019	0.035

and II where also the clearing temperatures T_c are indicated. η_{12} is calculated from η_{45° using

$$\eta_{12} = 4 \eta_{45^\circ} - 2(\eta_1 + \eta_2). \quad (19)$$

The results are given in figure 9 for N4 only.

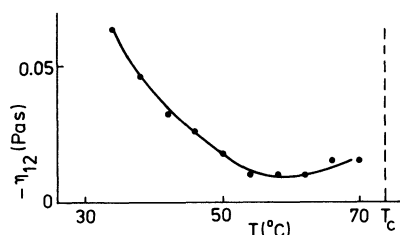


Fig. 9. — Shear-viscosity η_{12} of N4.

With the flow-alignment set-up θ_0 has been measured for N4 and DIBAB (see Fig. 10 and tables I and II). The errors due to the assumption $\sin^2 \theta \ll 1$ (eq. (17)) are smaller than the experimental errors. In addition p,p'-octylcyanobiphenyl (8CB) has been considered, for which Skarp *et al.* [15] found that for temperatures below $(T_c - 1)^\circ\text{C}$ no flow-alignment

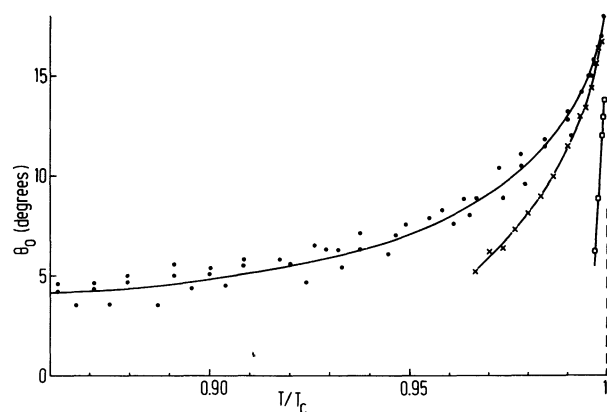


Fig. 10. — Flow-alignment angle θ_0 of N4 (●); DIBAB (×) and 8CB (□).

Table III. — Results for θ_0 of 8CB ($T_c = 40.1^\circ\text{C}$).

$T (^\circ\text{C})$	39.1	39.3	39.6	39.7	39.8
θ_0	6.2°	8.9°	12.0°	12.9°	13.8°

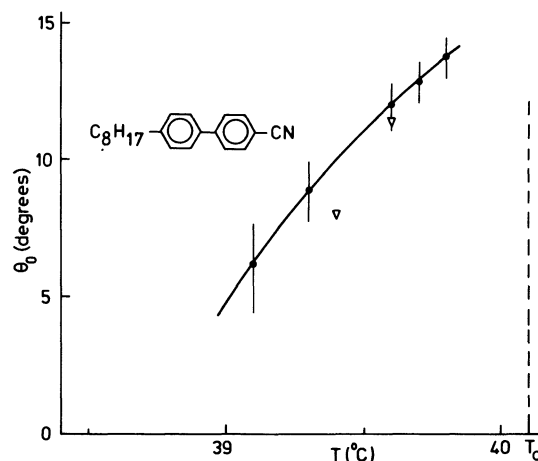


Fig. 11. — Flow-alignment angle θ_0 of 8CB on an expanded scale ; (▽) Skarp *et al.* [15].

exists. Our measurements (see Fig. 11 and table III) are in agreement with these results.

5. Discussion. — We have so far considered five viscosity coefficients. As already mentioned, the hydrodynamic theory of nematic liquid crystals involves six viscosity coefficients. In order to obtain the full set we have to rely on the Onsager-Parodi relation [18], which can be written in the form

$$\eta_1 - \kappa_1 = \eta_2 - \kappa_2. \quad (20)$$

In principle one can check this equation experimentally if we use additional results for the rotational viscosity $\gamma_1 = \kappa_1 + \kappa_2$ from Van Dijk *et al.* [9]. In practice, however, equation (20) is always fulfilled within the experimental accuracy due to the relatively large errors in η_1 . This is best illustrated when (20) is rewritten in quantities that are directly measurable :

$$\eta_1 = \eta_2 + \gamma_1 \left(\frac{1 + \tan^2 \theta_0}{1 - \tan^2 \theta_0} \right). \quad (21)$$

The results for η_1 calculated in this way and measured directly are compared in table IV. For N4 a comparison with direct measurements of η_1 and with the results from Knepe *et al.* [7] is given in figure 7. Application of equation (21) gives values for η_1 with errors of less than 5%. The results for η_1 of N4 and DIBAB obtained in this way are given in tables I and II.

We can also compare our results with visco-

Table IV. — *Validity of the Onsager-Parodi relation (Eq. (21)) for some compounds at 25 °C.*

Compound	η_1 (10^{-3} Pa.s)	
	direct	from $\eta_2, \gamma_1, \theta_0$
N4	170 ± 17	185 ± 3
DIBAB	55 ± 5	59 ± 1
MBBA	136 ± 6 ^(a)	135 ± 1 ^(a)
5CB	114 ± 5 ^(b)	109 ± 1 ^(b)

^(a) From Knepe *et al.* [6, 8] and Gähwiler [21].

^(b) From Knepe *et al.* [7, 8] and Skarp *et al.* [4].

elastic ratios from light-scattering methods by Van Eck *et al.* [10]. With light-scattering one obtains η_{splay}/K_1 , η_{twist}/K_2 and η_{bend}/K_3 . Here K_1 , K_2 and K_3 are the elastic constants for splay, twist and bend, respectively, while η_{splay} , η_{twist} and η_{bend} are the viscosities related to these deformations, given by

$$\eta_{\text{splay}} = \gamma_1 - (\eta_2 - \eta_1 + \gamma_1)^2/4\eta_2, \quad (22)$$

$$\eta_{\text{twist}} = \gamma_1, \quad (23)$$

$$\eta_{\text{bend}} = \gamma_1 - (\eta_2 - \eta_1 - \gamma_1)^2/4\eta_1. \quad (24)$$

The results for these ratios are compared in figures 12-14. When calculating the ratios for N4 the elastic constants from De Jeu *et al.* [19] were used, and for DIBAB K_1 and K_3 from De Jeu *et al.* [20] and K_2 from Van Dijk *et al.* [9]. Comparing the results we note that the visco-elastic ratios from light-scattering are in several cases higher than the results from flow-measurements, especially for η_{splay}/K_1 . From equations (22) and (23) one necessarily finds that $\eta_{\text{splay}}/\eta_{\text{twist}} \leq 1$, but from light-scattering it was found that $\eta_{\text{splay}}/\eta_{\text{twist}} > 1$. This means that the values for η_{splay}/K_1 from light-scattering are probably too high. In the case of N4 the results of η_{twist}/K_2 and η_{bend}/K_3 are in good agreement for both techniques.

Knepe *et al.* [7] have discussed the dependence of the viscosities of several nematics on the temperature (via an activation energy) and on the orientational order. In particular they observed that $\eta_i/\bar{\eta}$, where $\bar{\eta} = \frac{1}{3}(\eta_1 + \eta_2 + \eta_3)$, shows a rather universal behaviour. Our results for DIBAB fit into this general trend.

We conclude from our results that it is quite possible to determine with a reasonable accuracy a complete set of nematic viscosities from flow-measurements. Some complications arise with the geometry for η_1 because of unfavourable boundary effects. An additional measurement of the rotational viscosity γ_1 makes it possible to get around these problems in a simple way. Finally we note that Leslie has described the nematic viscosities with a set of coefficients $\alpha_1 \dots \alpha_6$, different from the more experimental ones used in this paper. Via the known relations (Ref. [2]) these can, if desired, be calculated from the results given.

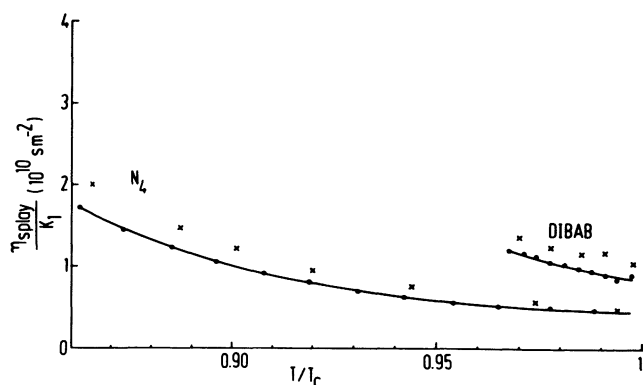


Fig. 12. — η_{splay}/K_1 of DIBAB and N4; (●) flow-measurements (this work); (×) light-scattering (ref. [10]).

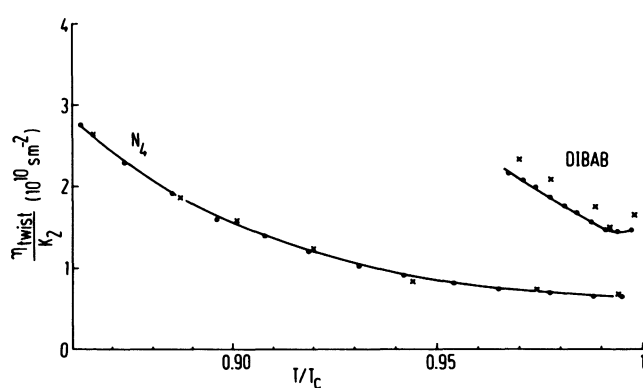


Fig. 13. — η_{twist}/K_2 of DIBAB and N4; (●) flow-measurements (this work); (×) light-scattering (ref. [10]).

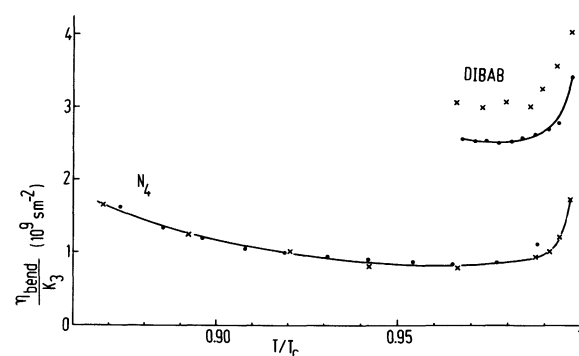


Fig. 14. — η_{bend}/K_3 of DIBAB and N4; (●) flow-measurements (this work); (×) light-scattering (ref. [10]).

Acknowledgments. — This work is part of the research program of the Stichting voor Fundamenteel Onderzoek der Materie (Foundation for Fundamental research on Matter-FOM) and was made possible with financial support from the Nederlandse Organisatie voor Zuiver Wetenschappelijk Onderzoek (Netherlands Organization for the Advancement of Pure Research-ZWO).

References

- [1] (a) ERICKSEN, J. L., *Mol. Cryst. Liq. Cryst.* **7** (1969) 153;
(b) LESLIE, F. M., *Arch. Ration. Mech. Anal.* **28** (1968) 265.
- [2] For reviews see : (a) LESLIE, F. M., *Advances in Liquid Crystals*, G. H. Brown, ed., Vol. **4** (Academic Press, New York) 1979, p. 1.
(b) DE JEU, W. H., *Physical Properties of Liquid Crystalline Materials* (Gordon and Breach, New York) 1980, Chap. 7.
- [3] GÄHWILLER, Ch., *Mol. Cryst. Liq. Cryst.* **20** (1973) 301.
- [4] SKARP, K., LAGERWALL, S. T. and STEBLER, B., *Mol. Cryst. Liq. Cryst.* **60** (1980) 215.
- [5] DE JEU, W. H., *Phys. Lett. A* **69** (1978) 122.
- [6] KNEPPE, H. and SCHNEIDER, F., *Mol. Cryst. Liq. Cryst.* **65** (1981) 23.
- [7] KNEPPE, H., SCHNEIDER, F. and SHARMA, N. K., *Ber. Bunsenges. Phys. Chem.* **85** (1981) 784.
- [8] KNEPPE, H., SCHNEIDER, F. and SHARMA, N. K., *J. Chem. Phys.* **77** (1982) 3203.
- [9] VAN DIJK, J. W., BEENS, W. W. and DE JEU, W. H., to be published.
- [10] VAN ECK, D. C. and WESTER, W., *Mol. Cryst. Liq. Cryst.* **38** (1977) 319.
- [11] HELFRICH, W., *J. Chem. Phys.* **51** (1969) 4092.
- [12] HELFRICH, W., *J. Chem. Phys.* **53** (1970) 2267.
- [13] MIESOWICZ, M., *Bull. Int. Acad. Pol. Sci. Math. Nat. Ser. A* (1936) 228.
- [14] FLÜGGE, S., *Handbuch der Physik* **8/2** (Springer-Verlag, Berlin) 1963.
- [15] SKARP, K., CARLSSON, T., LAGERWALL, S. T. and STEBLER, B., *Mol. Cryst. Liq. Cryst.* **66** (1981) 199.
- [16] CLADIS, P. E. and TORZA, S., *Phys. Rev. Lett.* **35** (1975) 1283.
- [17] LESLIE, F. M., *Q. J. Mech. Appl. Math.* **19** (1966) 357.
- [18] PARODI, O., *J. Physique* **31** (1970) 581.
- [19] DE JEU, W. H., LEENHOUTS, F. and POSTMA, F., *Advances in Liquid Crystal research and applications*, edited by L. Bata (Pergamon, Oxford) 1980.
- [20] DE JEU, W. H. and CLAASSEN, W. A. P., *J. Chem. Phys.* **67** (1977) 3705.
- [21] GÄHWILLER, Ch., *Phys. Rev. Lett.* **28** (1972) 1554.
-